2014

Solar Energy Harvesting Clear Glass For Building-integrated Photovoltaics

Kamal Alameh
Edith Cowan University

Mikhail Vasiliev
Edith Cowan University

Ramzy Alghamedi
Edith Cowan University

Mohammad Alam
Edith Cowan University

V. Rosenberg

Solar Energy Harvesting Clear Glass for Building-Integrated Photovoltaics

Kamal Alameh[1], Mikhail Vasiliev[1], Ramzy Alghamedi[1], Mohammad Nur-E-Alam[1] and Victor Rosenberg[2]

[1]Electron Science Research Institute, Edith Cowan University, Joondalup, WA 6027, Australia
[2]Tropiglas Technologies, Ltd, Western Australia
Email:k.alameh@ecu.edu.au

Abstract— We propose and demonstrate the concept of an energy-harvesting clear glass panel based on the use of all-inorganic luminophores embedded into a lamination layer in conjunction with low-emissivity coatings and CIS solar cells. Most of the visible solar radiation is transmitted through the laminated glass panel while UV radiation is down-converted and guided together with a part of infrared radiation to the edges for conversion to electricity by solar cells integrated at the edges of the glass panel. Experimental results demonstrate that a 10cmx10cm energy-harvesting clear glass can pass about 70% of the visible solar radiation, block 90% of UV and IR solar energy blocking and generate almost $30W_p/m^2$.

Keywords—Solar energy, luminophores, thin film coating.

I. INTRODUCTION

Renewable energy has been globally recognised as one of the most efficient approach for energy supply while directly addressing CO_2 emissions reduction. Photovoltaics (PV), the conversion of solar radiation to electricity, is currently the fastest-growing technology for electricity generation [1], and solar cell installations are expected to reach 200 GW p.a. by 2030. With 20% of the world's total energy consumption delivered for civil applications (consumers, residential and commercial) [2], energy efficient buildings have become very attractive, and currently building industry regulations are introducing special energy-efficiency requirements for renewable energy resources [3]. Our Electron Science Research Institute in conjunction with Tropiglas Technologies, Western Australia, has pioneered research and development activities on "energy-saving and energy-producing solar windows", aiming at providing a way of enhancing city-based building-integrated PV (BIPV) energy outputs, simultaneously with reducing the cooling- and heating-related energy consumption in buildings located in hot and moderate climates. Various low-emissivity (low-e) glass windows that are currently used inside buildings worldwide offer heat insulation, energy savings, and ultraviolet (UV) protection. In hot climates, cooling-related energy savings can be achieved in buildings employing low-e glass window panels that cover vast areas of walls and roofs, thus achieving significant economic benefits. More effective energy saving can be achieved by using window glazings in city buildings of tomorrow that offer a combination of properties, making it both energy-preserving (due to the blocking of infrared-range transparency) and also energy-generating (by efficiently convert the invisible solar energy into electricity). Future energy-efficient buildings will be either fully grid-independent, or possessing significant autonomous energy-generation capabilities. As modern city buildings typically have large window areas and small roof surface areas, the maximum power output that can be generated through conventional roof-mounted solar panels is limited, in comparison with the power that can be generated from solar windows. Sunlight contains a strong IR radiation flux, and by using high efficiency PV solar cells, energy-harvesting windows could generate considerable electricity. New energy harvesting clear glass windows are therefore key elements of BIPV systems, which address the future goal of achieving net zero energy consumption in buildings. Luminescent Solar concentrator (LSC) [4-6] is currently considered as a potential BIPV technology [4], even though attaining high transparency as well as high-efficiency remains challenging due to the limited availability of efficient IR luminophores. Organic-dyes-based LSCs have been used to absorb sunlight and re-emit it at a wavelength band at which solar cell efficiency is maximal [5-8]. However, for such LSCs, the overlap of absorption and emission of the organic dyes lowers the waveguiding capabilities of the concentrator, thus reducing its stability [6]. In addition, all reported LSC structures reported to date have the following major limitations [9, 10]:

- limited concentrator-area due to photon re-absorption within the light-guiding structure;
- low conversion efficiency, due to the unavailability of materials possessing efficient IR-excitable luminescence [10].

In this paper, we report practical transparent BIPV "solar windows" based on the use of a combination of luminescence and geometric light-trapping effects and spectrally-selective components for direct light deflection. We demonstrate a 10cmx10cm 70%-transparency energy-harvesting clear glass capable of generating around $30W_p/m^2$ and blocking 90% of UV and IR solar energy.

II. ENERGY-HARVESTING CLEAR GLASS STRUCTURE

Fig. 1 shows the energy-harvesting clear glass structure capable of reflecting and redirecting the solar infrared rays. The structure employs two ultra-clear flat glass panes, a spectrally-selective low-e coating deposited onto the back surface and a luminescent laminating interlayer comprising inorganic luminophores for wavelength conversion and light scattering.
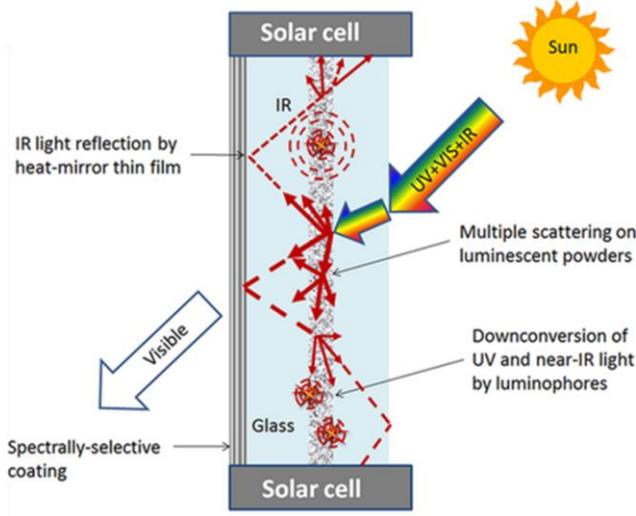
Fig.1. Schematic diagram of the energy-harvesting clear glass panel structure, which comprises two low-iron (Starphire UltraClear) flat glass panes, a spectrally-selective low-e coating deposited onto back surface and a luminescent interlayer containing inorganic luminophores.

II.A. LOW-EMISSIVITY THIN FILM COATINGS

The thin film interference-coating, shown in Fig. 1, was especially designed, using OptiLayer software package. It employed two metal layers and 5 dielectric layers which were developed using an e-beam/thermal evaporation system. Fig. 2 shows the modelled and measured transmission and reflection spectra of the metal/dielectric low-e thin film.
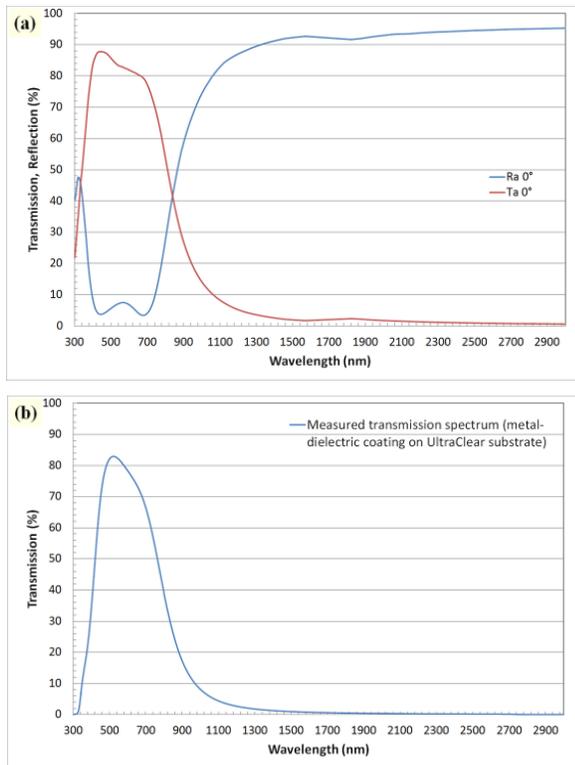

Fig.2. (a) Modelled (using optiLayer software package) transmittance and reflectance spectra of the optical interference coating designed to serve as a "heat mirror" and composed of 7 layers containing three different optical materials, (b) measured transmission spectrum of the developed thin-film.

The heat-mirror-film design of Fig. 2 was adjusted in terms of materials selection and number of layers deposited to ensure coating durability. Multiple coatings of this type were deposited onto $100 \times 100 \times 6 mm^3$ low-iron (Starphire UltraClear) glass substrates following the methods described in [11]. The thicknesses of all deposited thin film layers were measured in situ in real-time during deposition, using a custom-made laser reflectometer in conjunction with a quartz crystal microbalance pre-calibrated by the reflectometer [12]. Following this, a 10 mm glass pane was cleaned and used as a cover plate for a functionalized lamination interlayer.

II.B. FUNCTIONALIZED LUMINESCENT INTERLAYERS

To improve the efficiency of light collection within the light-trapping glass structures while maintaining a transparent all-inorganic solar concentrator, we embedded inorganic luminophore mixes into a transparent lamination layer. Four different all-inorganic luminophore powder types (described in Table 1) were finely grounded and different concentrations were used to investigate the optimum mix and powder concentrations that maximize the generated electricity while maintaining an adequate transparency (~70%).

Table1. Luminescent materials used for the functionalized interlayer

Phosphor ID	Luminophore composition type	Excitation/Emission wavelength bands
a	ZnS : (Ag, Tm)	**Ex:** 300-430 nm **Em:** near 795 nm
b	Y_2O_3 co-activated with several rare-earth ions and sensitized with Yb^{2+}.	**Ex:** mainly between 980 ± 40 nm **Em:** 1000 ± 50 nm and some visible upconversion emissions excited by 980 ± 40 nm
c	YPO_4:Nd	**Ex:** 940-980 nm **Em:** near 1060 nm
d	(Zn, Cd)S : Cu	**Ex:** 300-550 nm **Em:** near 940 nm

The rare-earth-doped Y_2O_3-based luminophore powder upconverted near 980 nm emissions to the visible range, and its near-IR emissions in the range 1000-1060 nm fairly matched the high-efficiency spectrum range of the $CuInSe_2$ (CIS) solar cells used. The (Zn, Cd)S:Cu luminophore efficiently converted a fraction of sunlight from (300-550) nm into (840-1040) nm. The absence of overlapping between the excitation and emission wavelength bands for both (Zn, Cd)S:Cu and Y_2O_3-based luminophores effectively reduced the energy losses linked to reabsorption.

The preparation steps for the functionalized interlayer are illustrated in Fig. 3 and summarized as follows: (i) powder grinding, (ii) powder weighing, (iii) powder-epoxy mixing, (iv) ultrasonic homogenization and particle agglomeration prevention, (v) agglomerate filtering through membrane filtration, (vi) liquid-phase lamination layer development, (vii) cover-glass application and (viii) epoxy UV curing.

Partial concentrations of luminophores (measured in wt%) were selected carefully in order to maintain the balance haziness of the samples, high transparency, and increasing scattering for efficient light routing to the glass panel edges.
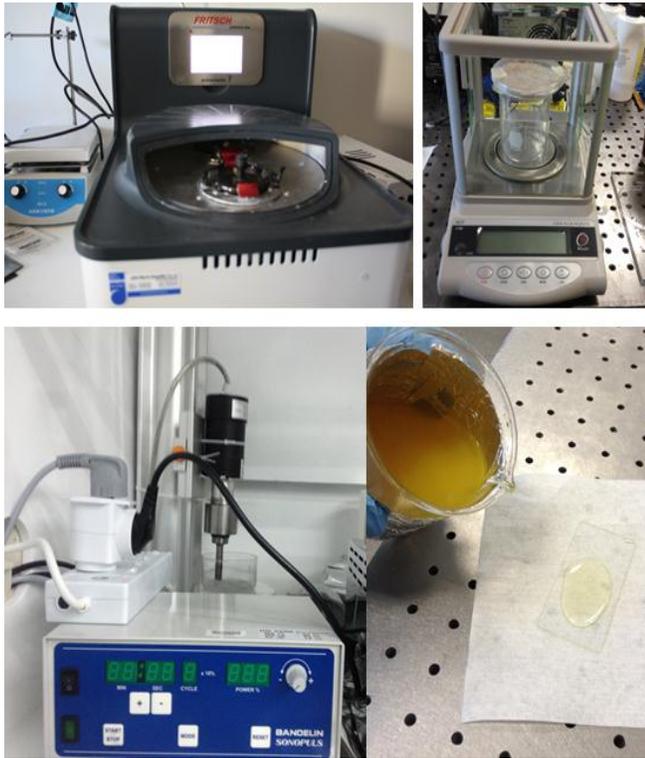

Fig.3. Preparation steps used for the development of functionalized luminescent interlayers – powder grinding, microbalance weighing, ultrasonic homogenisation followed by membrane filtration and liquid-phase interlayer dispensing.

The mean powder size varied between 0.5-2.5 μm after dry grinding for several hours inside Fritsch Pulverisette Premium Line 7 ball mill, and the solubilities of the various powders inside the optical epoxy varied with the material type and particle size. However, it was possible to form 1-2mm thick interlayers containing up to 0.1-0.3 wt% of total powder concentration with both Norland NOA61 and Wan Ta Shing 0049 single-component clear epoxies.

After UV curing of the epoxy, 9.2%-efficiency (at 25ºC), 60%-fill-factor CIS solar cell modules of size 100mmx25 mm were glued to the four edges of the 100mmx100mm glass panel and connected in parallel with some blocking diodes. Each CIS module had a saturated open-circuit voltage (Voc) near 7.8 V. Their Nominal Operating Cell Temperature (NOCT) is 47 °C and the temperature coefficient of output power 0.31 %/°C. Silicon cells were not used because of their limited spectral range (below 1100 nm) and instability with respect to shading effects.

II.C POWDER MIX OPTIMIZATION

Several energy harvesting clear glass samples were assembled with various luminophore compositions,

concentrations and thicknesses. We particularly designed the concentrator and interlayer characterization experiments to determine the maximum energy conversion and best routing capability. The generated electrical power levels for all samples were measured by illuminating the glass with a normally-incident, 2-inch collimated (and also diffused) solar simulator beam spectrally equivalent to AM1.5G irradiation, as shown in Fig. 5(a). A reference powder-free sample was also developed to benchmark the performances of all other samples. To characterize the relative flux-deflection capability, we defined the "Area Collection Gain" (*ACG*) parameter as follows:

$$ACG = 100\% * (I_{sc, sample} * V_{oc, sample} - I_{sc, ref} * V_{oc, ref})$$
$$/ (I_{sc, ref} * V_{oc, ref}) \quad \dots\dots\dots\dots\dots\dots\dots\dots\dots\dots \quad (1)$$

which evaluates the normalized difference between the measured electric output of the investigated sample and the powder-free reference sample.

III. RESULTS

Figure 4(b-d) summarizes the results of performance testing experiments performed with 8 samples (1-8), each containing an interlayer of different powder concentration. The measured ACG for each sample varied with the luminophore type used, luminophore compositions, powder concentrations and interlayer thickness.
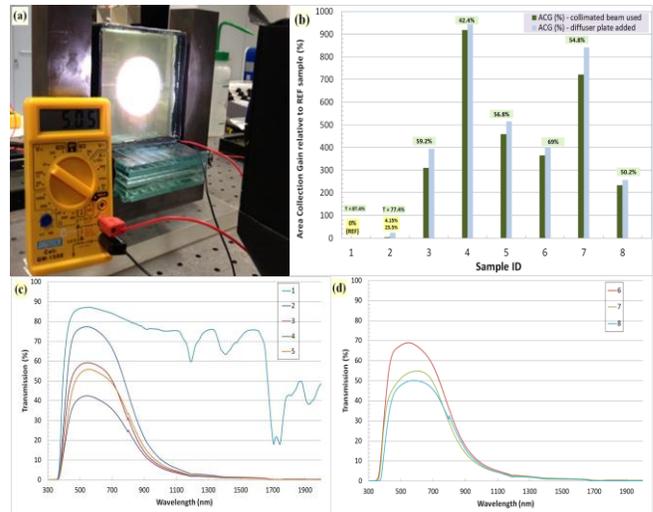

Fig.4. (a) Sciencetech Inc. solar simulator used to illuminate the glass collector area of samples at normal incidence with an AM1.5G beam of 2-inch diameter, (b) measured ACG and peak transparency data for the different samples; (c,d) measured transmission spectra for the various samples.

Only empirical optimisation of light scattering intensity, light collection efficiency and transparency was carried out, since the computation of the many factors affecting the concentrator performance could not be realistically predicted computationally. Sample 4 (see Fig. 4) contained three different powders which provided a combination of wide

excitation bands placed in the UV, blue and also the near-IR wavelength regions, a large Stokes shift and IR-range emission bands within the high responsivity wavelength range of CIS cells. On the other hand, sample 7 showed the best performance in peak outdoor illumination conditions (measured Isc = 60.5 mA; Voc = 7.4 V and thus Pout = 268.6 mW). When placed vertically, all samples intercepted solar flux of about 700 W/m2 * 0.01m2 = 7W, which results in a total optical-to-electrical conversion efficiency to η = 3.8%. To our knowledge, this result is remarkable for a solar concentrator of 55% transparency employing inorganic-only luminophores.

The optimized interlayer composition was also used to build an up-scaled 200mmx200mm energy harvesting clear glass sample. Fig. 5 shows typical I-V curves of our 100mmx100 mm and advanced 200mmx200 mm samples measured at "average" and peak outdoor illumination conditions, respectively.
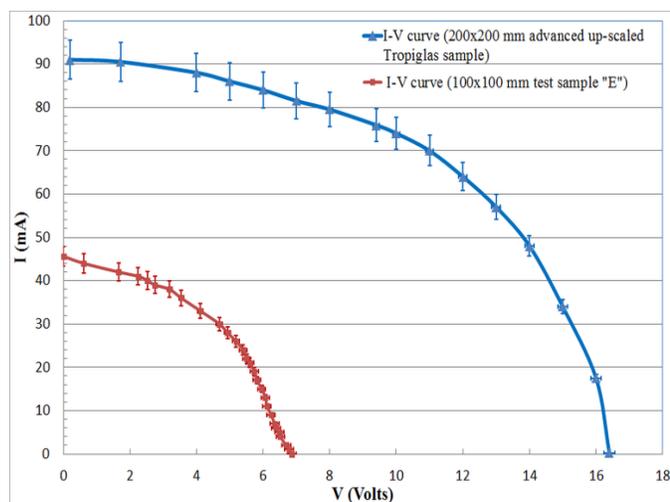

Fig.5. Measured I-V curves of optimized 200mx200mm energy harvesting clear glass samples at peak outdoor illumination conditions, and 100x100 mm sample (E) measured outdoors during average insolation conditions. Both samples were oriented vertically.

The thermal insulation and solar heat shielding performance of glazing systems employing low-emissivity high spectral selectivity solar-control coatings of our design (Fig 2) were characterized using LBNL's Optics 6.0 and WINDOW 6.3 software packages. The solar heat gain coefficient (SHGC) is near 0.41, making these samples among the industry-leading concentrators in terms of solar control performance, bearing in mind that the Light-to-Solar Gain (LSG) parameter is >1.8. The relatively high SHGC of 0.41 is mainly due to the high transparency of the sample. The calculated U-factor was < 1.8 W/(m^2 °K) for insulating glass units with a 0.5-inch air space.

IV. CONCLUSION

We have proposed and demonstrated the concept of a new energy-harvesting clear glass panel employing all-inorganic luminophore-doped epoxy resin interlayer in conjunction with spectrally-selective thin-film coatings and CIS PV solar cells. Experimental results have demonstrated an energy-harvesting laminated clear glass 10cmx10cm module possessing about 70% visible-range transparency, about 10% UV and IR energy transmission, about 10%, and around 30W/m2 power generation at peak solar illumination conditions.

REFERENCES

[1] M. A.Green, "Third generation photovoltaics: advanced solar energy conversion", 2003, Springer.

[2] International Energy Outlook 2013, a report by U.S. Department of Energy (2013), Chapter 6, p. 111, http://www.eia.gov/forecasts/ieo/pdf/0484(2013).pdf (sighted in March 2014).

[3] Zero Carbon Australia Stationary Energy Plan, published by The University of Melbourne Energy Research Institute, 2010, available from http://www.sustainable.unimelb.edu.au/files/mssi/MEI_Stationary-Energy-Report_2010.pdf (sighted in March 2014).

[4] V. Baranov, "Theoretical basis for the development of selective sunshade glazing," Provisional Patent application text supplied by Tropiglas Technologies Ltd, private communication.

[5] J. Batchelder, A. Zewail, and T. Cole, "Luminescent solar concentrators. 1: Theory of operation and techniques for performance evaluation," Appl. Opt., 18, 3090-3110 (1979).

[6] J. Batchelder, A. Zewail, and T. Cole, "Luminescent solar concentrators. 2: Experimental and theoretical analysis of their possible efficiencies," Appl. Opt., 20, 3733-3754 (1981).

[7] S. A. Evenson and A. H. Rawicz, "Thin-film luminescent concentrators for integrated devices," Appl. Opt., 34, 31, 7231-7238 (1995).

[8] S. A. Evenson and A. H. Rawicz, "Thin-film luminescent concentrators for integrated devices: a cookbook," Appl. Opt., 34, 31, 7302-7306 (1995).

[9] W. G. J. H. M. van Sark, K. W. J. Barnham, L. H. Slooff, A. J. Chatten, A. Buchtemann, A. Meyer, S. J. McCormack, R. Koole, D. J. Farrell, R. Bose, E. E. Bende, A. R. Burgers, T. Budel, J. Quilitz, M. Kennedy, T. Meyer, C. D. M. Donega, A. Meijerink, and D. Vanmaekelbergh, " Luminescent Solar Concentrators – A review of recent results," Opt. Express, 16, 26, 21773-21792 (2008).

[10] M. G. Debije and P. P. Verbunt, "Thirty years of luminescent solar concentrator research: Solar energy for the built environment," Adv. Energy Mater., 2, 12-35 (2012).

[11] Y. El Mouedden, R. Alghamedi, M. Nur-E-Alam, M. Vasiliev, and K. Alameh, "Thin film coatings for solar and thermal radiation control prepared by physical vapour deposition," in High Capacity Optical Networks and Enabling Technologies (HONET 2012), pp. 083-086 (2012).

[12] Mikhail Vasiliev, Mohammad Alam, V.A. Kotov, Kamal Alameh, V.I. Belotelov, V.I. Burkov, and A.K. Zvezdin, "RF magnetron sputtered (BiDy)3(FeGa)5O12:Bi2O3 composite garnetoxide materials possessing record magneto-optic quality in the visible spectral region", OPTICS EXPRESS, Vol. 17, No. 22, pp. 19519- 19535, 2009.